Imputation-based fine-mapping suggests that most QTL in an outbred *chicken* Advanced Intercross Line are due to multiple, linked loci

Monika Brandt[*1], Muhammad Ahsan[†1], Christa F. Honaker[‡], Paul B. Siegel[‡], Örjan Carlborg[*]

Affiliations:

[*] Department of Medical Biochemistry and Microbiology, Uppsala University, 751 23 Uppsala, Sweden

[†] Division of Computational Genetics, Department of Clinical Sciences, Swedish University of Agricultural Sciences, 750 07 Uppsala, Sweden

[‡]Department of Animal and Poultry Sciences, Virginia Polytechnic Institute and State University, Blacksburg, VA 24061, USA

[1] Authors contributed equally to this work

Short running title:

Imputation based fine mapping in an AIL

Key words:

Imputation based association, advanced intercross line, Virginia chicken lines, QTL fine mapping

Article summary:

After 50 generations of bi-directional selection, the Virginia chicken lines display a 12-fold difference in bodyweight at 56 days of age. Birds from the high and low selected lines were crossed to found an Advanced Intercross Line, which has been maintained for 9 generations. Using high-density genotypes of the founders, we imputed genotypes in intercross birds that were only genotyped for a sparse set of markers. Using single and multi-marker association analyses, we replicated nine known body-weight QTL. Multiple statistically independent associations were revealed in eight of the QTL, suggesting that most are caused by multiple linked loci.

Corresponding author:

Name: Örjan Carlborg

Address: Department of Medical Biochemistry and Microbiology, Uppsala University

BMC, Box 582

SE-751 23 Uppsala

Phone: +46-18-4714592

Email: orjan.carlborg@imbim.uu.se

ABSTRACT

The Virginia *chicken* lines have been divergently selected for juvenile body-weight for more than 50 generations. Today, the high- and low-weight lines show a 12-fold difference for the selected trait, 56-day body-weight. These lines provide unique opportunities to study the genetic architecture of long-term, single-trait selection. Previously, several Quantitative Trait Loci (QTL) contributing to weight differences between the lines were mapped in an F_2-cross between them, and these were later replicated and fine-mapped in a nine-generation advanced intercross of them. Here, we explore the possibility to further increase the fine-mapping resolution of these QTL via a pedigree-based imputation strategy that aims to better capture the haplotype-diversity in the divergently selected, but outbred, founder lines. The founders of the intercross were high-density genotyped, and then pedigree-based imputation was used to assign genotypes throughout the pedigree. Imputation increased the marker-density 20-fold in the selected QTL, providing 6911 markers for the subsequent analysis. Both single-marker association and multi-marker backward-elimination analyses were used to detect associations to 56-day body-weight. The approach revealed several statistically and population-structure independent associations and increased the resolution of most QTL. Further, most QTL were also found to contain multiple independent associations, implying a complex underlying architecture due to the combined effects of multiple, linked loci on independent haplotypes that still segregate in the selected lines.

INTRODUCTION

Long-term selective breeding of animals and plants for extreme phenotypes has resulted in genetically distinct lines that are a valuable resource for dissecting the genetic architecture of complex traits (Hill 2005). Most traits of interest in animal breeding (e.g. production of eggs or meat, resistance to disease) are influenced by a combination of genetic and environmental

64 factors. Due to their multi-factorial nature and despite the ability to obtain data on both
65 genome-wide genetic markers and phenotypes from large numbers of individuals, it is
66 challenging to disentangle their genetic architecture when working with commercial
67 populations. An alternate strategy is to make use of experimental populations resulting from
68 long-term selection experiments, where the focus has been to develop divergent lines from a
69 common base-population using more coherent selection criteria. Such populations will
70 display larger phenotypic differences than populations subjected to composite, commercial
71 breeding programs and hence facilitate in-depth studies of the genetic basis underlying the
72 selection-response and general genetic architecture of these traits (Andersson and Georges
73 2004). Given that many of the agriculturally important traits relate to metabolism, feeding-
74 behavior and growth, they also provide a good model for translational studies to decipher the
75 genetic architecture of traits of interest in human medicine, including obesity, eating
76 disorders, and diabetes (Andersson 2001).
77
78 The Virginia lines are experimental populations established in 1957 to study the genetic
79 effects of long-term (more than 50 generations), divergent, single-trait selection for 56-day
80 high (HWS) or low (LWS) body-weight in *chickens* (Dunnington and Siegel 1996; Márquez
81 *et al.* 2010; Dunnington *et al.* 2013). The lines originated from the same base population,
82 composed by crossing seven partially inbred White Plymouth Rock *chicken* lines, and today
83 display a 12-fold difference in body-weight at 56 days of age (Márquez *et al.* 2010;
84 Dunnington *et al.* 2013). In addition to the direct effects of selection on body-weight, the
85 selected lines also display correlated selection responses for a range of metabolic and
86 behavioral traits including disrupted appetite, obesity, and antibody response (Dunnington *et*
87 *al.* 2013).
88

89 The Virginia HWS and LWS lines have been used extensively for studying the genetic
90 architecture of body-weight and other metabolic traits. These studies have uncovered a
91 number of loci with minor direct effects on body-weight, metabolic traits and body-stature
92 traits by Quantitative Trait Loci (QTL) mapping in an F_2 intercross (Jacobsson *et al.* 2005;
93 Park *et al.* 2006; Wahlberg *et al.* 2009). Also, a network of epistatic loci has been found to
94 make a significant contribution to long-term selection response through the release of
95 selection induced additive variation (Carlborg *et al.* 2006; Le Rouzic *et al.* 2007; Le Rouzic
96 and Carlborg 2008). Explorations of the genome-wide footprint of selection by selective-
97 sweep mapping suggests that perhaps more than one hundred loci throughout the genome
98 have contributed to selection response (Johansson *et al.* 2010; Pettersson *et al.* 2013), and
99 many of these contribute to 56-day body weight (Sheng *et al.* 2015).
100
101 To replicate and fine-map the body-weight QTL inferred in the F_2 intercross, we developed,
102 genotyped and phenotyped, for body-weight at 56 days of age (BW56), a nine-generation
103 Advanced Intercross Line (AIL). This large AIL originated from the same founders as the F_2
104 intercross, but was selectively genotyped at a higher resolution (~1 marker/cM) in nine QTL
105 (Besnier *et al.* 2011). In this population, most of the original minor (Besnier *et al.* 2011) and
106 epistatic (Pettersson *et al.* 2011) QTL were replicated and fine-mapped. These earlier studies
107 analyzed the data using a haplotype-based linkage-mapping approach in a variance-
108 component based model framework to infer single-locus effects (Besnier *et al.* 2011) or a
109 fixed-effect model framework assuming fixed alternative alleles in the two founder-lines for
110 detecting epistasis (Pettersson *et al.* 2011). The variance-component model was used in the
111 replication study in order to avoid the assumption of allelic fixation in the founder-lines. By
112 implementing it in a Flexible Intercross Analysis (FIA) modeling framework (Rönnegård *et*

113 *al.* 2008), it was expected to improve power when the parental lines carry alleles with
114 correlated effects (e.g. multiple alleles with similar effects).
115
116 Although the initial studies mapped QTL under the assumption of fixation, or an effect
117 correlation, of divergent alleles in the crossed lines, the results at the same time implied that
118 multiple alleles might be segregating in several of the mapped regions. To this end, the first
119 QTL replication study in the AIL population (Besnier *et al.* 2011) found a large within
120 founder-line heterogeneity in the allelic effects. Later the selective-sweep studies, that utilized
121 data from multiple generations of divergently selected and relaxed lines, identified on-going
122 selection and multiple sweeps in many QTL (Johansson *et al.* 2010; Pettersson *et al.* 2013), as
123 well as extensive allelic purging (Pettersson et al. 2013). This allelic heterogeneity challenges
124 attempts to dissect the architecture of the selected trait via e.g. QTL introgression (Ek *et al.*
125 2012). Alternative approaches are therefore needed to uncover multi-locus, multi-allelic
126 genetic architectures in QTL and their contributions to the long-term response to directional
127 selection.
128
129 In this study, to explore an imputation-based association-mapping strategy for further
130 dissection of previously mapped and replicated QTL (Besnier *et al.* 2011; Pettersson *et al.*
131 2011), we made use of available high-density (60K SNP-Chip) genotypes for founders
132 (Johansson *et al.* 2010; Pettersson *et al.* 2013) and intermediate-density SNP-genotypes in
133 several QTL in the entire 9-generation AIL-pedigree. By increasing the marker-density in the
134 QTL throughout the AIL by imputation, we aimed to better capture the segregating
135 haplotypes within and between the divergently selected founder populations than with the
136 previously used markers. This aim can be achieved as the original markers genotyped in the
137 AIL were selected to identify high- and low-line derived alleles, and not alleles that segregate

within or across the founder lines. By testing for association between imputed markers and body-weight, the fine-mapping analyses were less constrained by the original selection of markers and facilitated a more thorough exploration of the genetic architectures of the nine evaluated QTL. Our results show that the imputation-based approach not only allows replication of most QTL, but also that it is possible to utilize historical recombination in the pedigree to improve the resolution in the fine-mapping analyses. We found that several of the original QTL are likely due to the combined effects of multiple linked loci, several of which are segregating for alleles originating from different haplotypes in the founder population of the selected lines.

MATERIALS AND METHODS

Animals

The Virginia *chicken* lines are part of an ongoing selection experiment to study the genetics of long-term, single-trait selection (Márquez *et al.* 2010; Dunnington *et al.* 2013). It was initiated in 1957 from a base population, generated by intercrossing seven partially inbred lines of White Plymouth Rock *chickens*. From the offspring of the partially inbred lines, resulting from the intercrossing, the birds with the highest and lowest 56-day body-weights (with some restrictions), respectively, were selected to produce the high- and low-weight selected lines (HWS and LWS) (Márquez *et al.* 2010; Dunnington *et al.* 2013). Since then, the lines have undergone divergent selection for increased and decreased body weights with one new generation hatched in March of every year.

An Advanced Intercross Line (AIL) was founded by reciprocal crosses of 29 HWS and 30 LWS founder birds from generation 40 (Besnier *et al.* 2011). The mean, sex-averaged 56-day

163 body weights for HWS and LWS at this generation were 1522 g and 181 g, respectively.
164 Repeated intercrossing of birds was used to develop a nine-generation AIL consisting of
165 generations F_0-F_8. In each generation, approximately 90 birds were bred by paired mating,
166 genotyped, and weighed at 56 days of age (BW56). The exceptions were generations F_3 and
167 F_8 that contained 405 and 437 birds, respectively (Besnier *et al.* 2011). In total, the AIL
168 population consisted of 1529 F_0 to F_8 individuals with complete records on pedigree and
169 genotypes (see below), and 1348 F_2-F_8 individuals with juvenile body-weight (BW56)
170 records.
171
172 **Genotyping**
173 The complete AIL pedigree (1529 birds) had earlier been genotyped in nine selected QTL for
174 304 SNP-markers that passed quality-control as described in (Besnier *et al.* 2011). Further, 40
175 of the founders for the pedigree (20 HWS and 20 LWS) had also earlier been genotyped using
176 a whole genome 60K SNP chip (Johansson *et al.* 2010; Pettersson *et al.* 2013). The 6607
177 markers from the SNP-chip that were informative and passed quality control in that study are
178 located in the nine QTL-regions targeted in this study. When merging the information from
179 the 60K SNP chip and the information from the 304 markers genotyped earlier, 55 markers in
180 40 founders were genotyped using both methods. Out of these 55 markers, 28 markers with
181 genotype inconsistencies between the genotyping technologies were removed during quality
182 control. In total, our analyses were based on 6888 markers, where 40 of the 59 AIL founders
183 had genotypes for all markers, and the remaining individuals in the pedigree had genotypes
184 for 281 markers. Table 1 shows how these markers are distributed across the nine QTL
185 regions.
186
187

188 ***Table 1.*** *Genotyped and imputed markers across the nine analyzed QTL.*

GGA[a]	QTL[b]	Start[c] (bp)	End[c] (bp)	QTL Size (bp)	Markers AIL[d]	Markers 60k[e]	Markers Total[f]	Marker Density[g]
1	Growth1	169 634 954	181 087 961	11 453 008	26	504	530	46
2	Growth2	47 929 675	65 460 002	17 530 328	33	667	700	40
2	Growth3	124 333 151	133 581 122	9 247 972	19	395	414	45
3	Growth4	24 029 841	68 029 533	43 999 693	57	1885	1942	44
4	Growth6	1 354 213	13 511 203	12 156 991	23	514	537	44
4	Growth7	85 459 943	88 832 107	3 372 165	14	141	155	46
5	Growth8	33 696 791	39 052 438	5 355 648	5	221	226	42
7	Growth9	10 916 819	35 491 706	24 574 888	76	1397	1473	60
20	Growth12	7 109 709	13 899 993	6 790 285	28	883	911	134

189 *[a] Gallus Gallus Autosome [b] QTL names as in (Jacobsson et al. 2005); [c] Base pair position according to Chicken*
190 *genome assembly (galGal3) of May 2006; [d] Markers as in (Besnier et al. 2011); [e] Markers as in (Johansson et al.*
191 *2010); [f] Total markers in [d] and [e]; [g] Markers / Mb*

192

193 **Phasing and imputation of markers**

194 All genotyped markers in the QTL (Table 1) were first ordered according to their physical
195 location in the *Chicken* genome assembly of May 2006 (*galGal3*). In the ordered marker set,
196 the SNP-chip markers were evenly distributed in the intervals between the sparser set of
197 markers genotyped across the entire AIL.

198

199 Using the software ChromoPhase (Daetwyler *et al.* 2011), we phased and imputed genotypes
200 for the complete set of 6888 markers across the entire AIL pedigree. ChromoPhase first

phases large segments of chromosomes, in our case the QTL regions. It then imputes the missing genotypes in the AIL individuals genotyped with the sparse set of markers from the genotype information available in high-density genotyped founders utilizing the pedigree information. It thus predicts both phased haplotypes across the nine studied QTL and genotypes at markers that were only genotyped in a subset of the founder individuals in the pedigree.

Single-marker association analyses

The *qtscore* function in the GenABEL package (Aulchenko *et al.* 2007) was used to test for association between body-weight at 56 days of age and, genotyped or imputed, individual genetic markers within the targeted QTL. The allelic effect of each marker, $\hat{\beta}_{genotype}$, was estimated using a regression model (Model 1), where the genotype at each marker was coded in $\boldsymbol{Z}$ as 0 if homozygous for the major allele, 1 if heterozygous, and 2 if homozygous for the minor allele. Sex and generation was added as categorical covariates, with 2 different levels for sex and 7 different levels for generation, defined for each individual in $\boldsymbol{X}$. The phenotype, body-weight at 56 days of age, is given in the numerical variable **y**.

$$y = \mu + \beta_{sex,generation}X + \beta_{genotype}Z + \varepsilon \qquad \text{(Model 1)}$$

ε was assumed to be iid and normally distributed around 0 with variance σ^2. μ is the intercept, that in this model represented the mean body-weight at 56 days of age for female individuals from the F_2 generation.

Multi-locus association analysis accounting for population-structure

The single-marker association analyses based on Model 1 neither account for possible genetic dependencies (linkage or LD) between markers within the QTL regions, nor account for the potential effects of population-structure in the AIL (Peirce *et al.* 2008; Cheng *et al.* 2010). Earlier studies have shown that the genetic architecture of body-weight is highly polygenic in this population (Jacobsson *et al.* 2005; Wahlberg *et al.* 2009; Johansson *et al.* 2010; Besnier *et al.* 2011; Pettersson *et al.* 2011; 2013; Sheng *et al.* 2015) and we therefore implemented a statistical approach based on this. To correct for population-structure in the deep intercross line and identify an experiment-wide set of independent association-signals, we use a forward-selection/backward-elimination procedure in a bootstrap-based framework developed for this purpose (Valdar *et al.* 2009; Sheng *et al.* 2015). As all markers with genotypes could not be included in a backward-elimination analysis due to the limited sample size, we first used a forward-selection strategy to identify a smaller set of statistically suggestive independent signals within each QTL region to be thoroughly evaluated in the backward-elimination analysis (Valdar *et al.* 2009; Sheng *et al.* 2015). The forward-selection analysis was performed by scanning across all markers within each QTL using Model 1. If any of the markers were nominally significant ($p < 0.05$) in the scan, the marker with the strongest association was added as a covariate in the model. This procedure was repeated until no more significant markers were detected. The models were fitted using the *qtscore* function in the *GenABEL* package (Aulchenko *et al.* 2007) as described previously. The markers from this analysis with an allele-frequency > 0.10 in the population were subjected to the full backward-elimination analysis described below.

In short, we used a bootstrap based backward-elimination model-selection framework (Sheng *et al.* 2015) across the markers selected by forward-selection in the QTL. An adaptive model selection criterion controlling the False Discovery Rate (Abramovich *et al.* 2006; Gavrilov *et*

al. 2009) was used during backward-elimination in a standard linear model framework, starting with a full model including the fixed effects of sex and generation, and the additive effects of all markers (Model 2). :

$$y = \mu + \beta_{sex,generation,markers}X + \varepsilon \quad \text{(Model 2)}$$

where phenotype, sex, and generation are coded as described for model 1 and where ε again is assumed to be iid and normally distributed around 0 with variance σ^2. The intercept, μ, represents the mean body-weight at 56 days of age for female individuals from the F_2 generation. In model 2, genotypes are coded based on the line-origin of the alleles at each locus. If an individual was homozygous for the major allele in the AIL-founders from the high-weight selection line, its genotype was coded as 1 at that locus. If an individual was heterozygous, its genotype was coded as 0. If an individual was homozygous for the allele corresponding to the major allele in AIL-founders from the low-weight selection line, its genotype was coded as -1. By coding genotypes in a -1, 0, and 1 manner, the estimates, $\hat{\beta}_{marker}$, from fitting model 2 will be negative if a weight-decreasing allele is derived from the high-weight line or if a weight-increasing allele is derived from the low-weight line.

Convergence was based on a 20% FDR level. The analysis was performed using bootstrapping with 1000 resamples. Markers with an RMIP (Resample Model Inclusion Probability) > 0.46, as suggested for an AIL generation F_{18} (Valdar *et al.* 2009), was included in the final model. The FDR in the final model was confirmed using the original FDR procedure described in (Benjamini and Hochberg 1995) as implemented in the p.adjust function in the R stats-package (R Development Core Team 2015). The additive genetic effect for each locus was estimated using the multi-locus genetic model described above (Model 2).

Data availability

Genotype and pedigree data will be included as supplementary information in the published version of the manuscript.

RESULTS AND DISCUSSION

We compared the results of the imputation-based association analyses with the previously reported results from the linkage-based analysis of the same nine QTL in Besnier *et al.* (2011). Figure 1 shows the statistical support for association and linkage to BW56 across the QTL. As the imputation-based analysis does not model pedigree-relationships, comparisons were made to the results from model A in (Besnier *et al.* 2011). Overall, the results between the two analyses overlap well. For several of the QTLs, we were able to fine-map the associated regions using imputed genotypes for SNPs within these regions. The overall results from the single-marker association analyses also agree with those from the bootstrap-based forward-selection/backward-elimination approach used to identify genome-wide independent association signals.

Four statistically independent associated markers in the GGA7 QTL *Growth9*

The QTL *Growth9* on GGA7 (Gallus Gallus Autosome 7) (Figure 1; 10.9-35.5 Mb) was the only QTL that reached genome-wide significance in the first F_2 intercross between the HWS and LWS lines (Jacobsson *et al.* 2005). It was later identified as a central locus in an epistatic network explaining a large part of the difference in weight between HWS and LWS lines (Carlborg *et al.* 2006). In the earlier fine-mapping analysis, the linkage signal covers most of the QTL region (from 15-35 Mb), but further analyses showed that two independent loci were segregating in the region (Besnier *et al.* 2011). The signal in the imputation-based association

analysis performed here is more focused, with a highly significant signal in a 2.8 Mb region between 23.7-26.4 Mb that overlaps with the strongest signal in the linkage-scan. Previously, Ahsan *et al.* (2013) explored potential candidate mutations in the QTL and found two regulatory SNPs near the peak at 21 Mb (21.6 and 22.7 Mb) and a synonymous-coding SNP in a CpG island in an exon of the Insulin-like growth factor binding protein 2 *(IGFBP2)* gene in the middle of the major association peak at 24.8 Mb. In addition to the strong association around 24 Mb, the association analysis also highlights two additional regions (centered around 18 Mb and 29 Mb) that are also shown to be experiment-wide independent signals in the backward-elimination analysis. The second QTL detected in the linkage analysis (*Growth9.2*) was only nominally significant in the single-marker association analysis, but as a marker in this region was included in the final model from the bootstrap-based backward-elimination analysis this suggests that the effect of this locus might be dependent on the genotype at other loci. In Table 2, we provide the additive effects and the significance of the experiment-wide independent loci from the backward-elimination analysis.

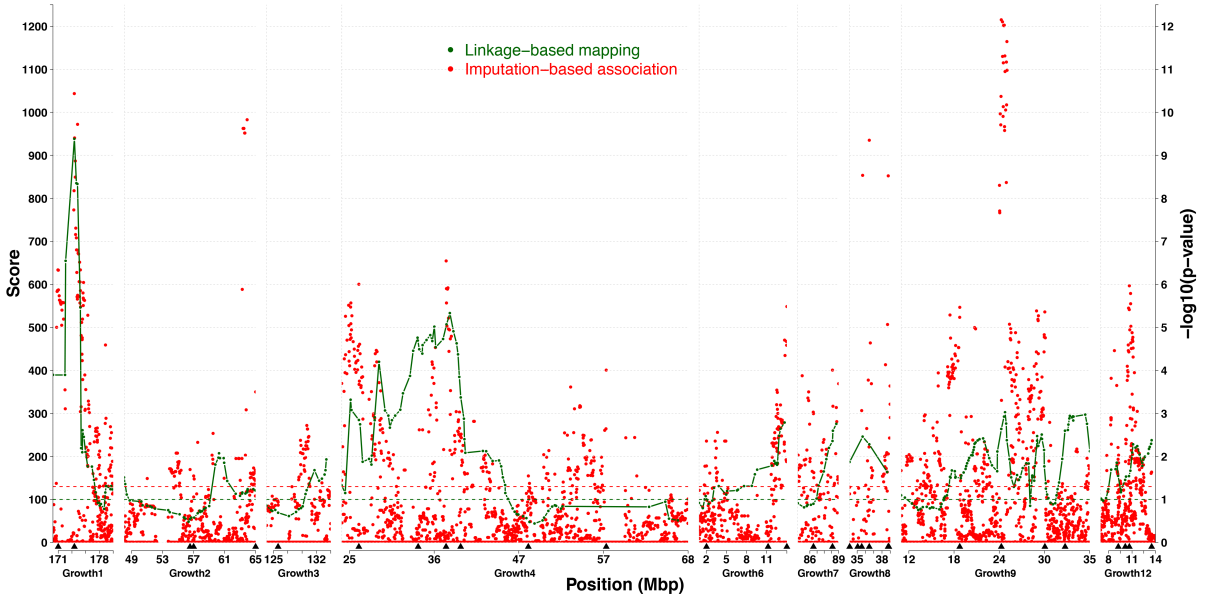

Figure 1. *Comparison between linkage and association-based fine-mapping analyses of nine QTL in an Advanced Intercross Line chicken population. Green lines show the statistical support curve (score statistics from model A) for the linkage-based mapping study of Besnier et al. (2011) and the red dots associations to*

each analyzed marker in the new imputation-based association analysis (this study). The green and red horizontal dotted lines indicates the significance thresholds for the linkage-analysis threshold and the nominal significance threshold in the imputation-based association analysis, respectively. Arrowheads under the x-axis indicate the position of markers identified as experiment-wide significant in the bootstrap-based backward-elimination procedure.

Table 2. *Estimated additive effect and standard error for experiment-wide independent association signals, between body-weight at 56 days of age and genotype, identified in a bootstrap based approach implemented in a backward-elimination model-selection framework across the markers in the genotyped QTL. For a marker with a positive estimated additive effect, the effect on weight is caused by the allele with its origin in the line associated with the sign of the effect, i.e. an allele with its origin in high-line is associated with an increase in body-weight and an allele with its origin in low-line is associated with a decrease in body-weight. In cases where a weight-increasing allele has its origin in the low-line or a weight-decreasing allele has its origin in the high-line the sign of the estimated additive effect will be negative.*

GGA[a]	QTL[b]	Position[c] (bp)	Marker[d]	a ± SE.[e]	Sign[f]
1	*Growth1*	170 637 618	rs13968052	16.3 ± 6.6	1.3×10^{-2}
		173 709 608	rs14916997	19.3 ± 5.5	4.8×10^{-4}
2	*Growth2*	56 720 515	rs14185295	13.2 ± 6.2	3.3×10^{-2}
		57 198 629	rs14185836	-12.1 ± 6.2	5.4×10^{-2}
		65 460 002	rs14196021	14.0 ± 5.9	1.7×10^{-2}
2	*Growth3*	126 000 254	rs16120360	12.6 ± 5.8	3.0×10^{-2}
3	*Growth4*	26 215 175	rs14328509	19.8 ± 5.4	2.3×10^{-4}
		33 743 569	rs314044798	-21.9 ± 6.1	3.8×10^{-4}
		37 287 334	rs316425755	27.8 ± 6.9	5.7×10^{-5}
		39 139 081	rs15468467	27.0 ± 7.3	2.1×10^{-4}
		47 729 342	rs316384373	-13.1 ± 6.8	5.5×10^{-2}
		57 624 596	rs14363139	18.2 ± 4.1	2.9×10^{-4}

4	*Growth6*	2 392 397	rs14419462	19.7 ± 7.6	1.0×10^{-2}
		10 914 312	rs14428120	-14.5 ± 5.8	1.3×10^{-2}
		13 511 203	rs15500313	17.7 ± 6.0	3.4×10^{-3}
4	*Growth7*	86 755 267	rs14499758	18.1 ± 6.3	3.9×10^{-3}
		88 325 118	rs15639000	13.4 ± 5.4	1.3×10^{-2}
5	*Growth8*	33 713 055	rs14530756	-13.5 ± 5.3	1.1×10^{-2}
		34 772 650	rs16487762	15.0 ± 6.8	2.7×10^{-2}
		35 299 978	rs16487933	-18.6 ± 6.0	1.8×10^{-3}
		36 291 277	rs13585490	14.1 ± 5.3	7.3×10^{-3}
		38 774 986	rs315605733	23.3 ± 7.3	1.4×10^{-3}
		38 867 279	rs314075508	16.4 ± 5.5	3.0×10^{-3}
7	*Growth9*	18 544 622	rs14611566	-20.1 ± 5.1	9.4×10^{-5}
		23 959 214	rs16596357	18.9 ± 5.6	7.7×10^{-4}
		29 631 963	rs10727581	15.9 ± 6.1	9.0×10^{-3}
		32 262 733	rs317586448	-13.2 ± 5.0	8.7×10^{-3}
20	*Growth12*	9 302 754	rs14277526	21.8 ± 6.8	1.4×10^{-3}
		10 165 171	rs14278292	-14.7 ± 6.5	2.4×10^{-2}
		10 667 729	rs16172598	14.3 ± 5.1	5.1×10^{-3}
		13 427 530	rs16176151	8.5 ± 5.2	1.0×10^{-1}

[a]Gallus Gallus Autosome; [b]QTL name as in (Jacobsson et al. 2005) ;[c] Base pair position according to Chicken genome assembly (galGal3) of May 2006; [d] SNP name as in NCBI dbSNP ;[e]Additive effect ± Standard Error calculated in a model including all loci in the table; [f] Significance of the estimates additive genetic effect from fitting model 2 with the final set of markers selected in the bootstrap-based backward-elimination procedure.

Two statistically independent associated markers in the GGA1 QTL *Growth1*

The strongest association in the study by Besnier *et al.* (2011) was found on GGA1 in the QTL *Growth1* (Figure 1; 169.6-181.1 Mb). Here, the second strongest association was detected in that QTL. The imputation-based association analysis, however, highlights two

significant associations, separated by a region of very low association. The strongest of these association-peaks was located near the peak detected using the earlier linkage-based analysis. Several of the significant associated markers were located in this region (173.6 to 175.3 Mb). A candidate gene for growth, Asparagine-linked glycosylation 11 homolog gene *(ALG11)*, is located at 174.6 Mb and has a strong mutation in its regulatory region (Ahsan et al. 2013). The second association was found to a group of significant markers in a narrower region upstream from the main linkage-peak (170.3 and 171.7 Mb). The association analysis thus suggests that the original 10.6 Mb QTL region is due to the effects of two separate loci located in these confined 1.5 Mb and 1.8 Mb regions. This is further supported by the forward-selection/backward-elimination procedure, which identifies two experiment-wide independent signals to markers within *Growth1*, one at 170.6 Mb and one at 173.7 Mb.

Four statistically independent associated markers in the GGA2 QTLs *Growth2 and Growth3*

GGA2 contain two QTL. *Growth2* (Figure 1; 47.9-65.5 Mb) has one highly associated peak at 64.3 Mb. *Growth3* (Figure 1; 124.3-133.6 Mb) was the least significant QTL in the association analysis, with a small peak at 129 Mb. The forward-selection/backward-elimination analyses identify 3 significant associations in *Growth2* at 56.7 Mb, 57.2 Mb, and 65.5 Mb respectively, with the strongest significance at 65.5 Mb. This suggests that there are two distinct associated loci in *Growth2*. In the earlier linkage-based analysis the strongest signal in *Growth2* was found at 60.6 Mb. In *Growth3* the strongest signal detected here is shifted almost 4 Mb upstream from the top signal found in the earlier linkage-based analysis.

Six statistically independent associated markers in the GGA5 QTL *Growth8*

365 One of the strongest association signals was found on GGA5 in the QTL *Growth8* (Figure 1;
366 33.7-39.1 Mb). The most associated markers were located in the central part of this 5.3 Mb
367 QTL and overlaps with the earlier linkage-signal. The association signal was, however,
368 stronger than the linkage signal suggesting that the imputed markers tag the QTL better than
369 the haplotypes inferred from the sparser set of genotyped markers. The results from the
370 forward-selection/backward-elimination analyses (Table 2) suggest that several markers tag
371 the variation present in this region and the strongest associated SNP was located at 38.7 Mb.
372
373 **Six statistically independent associated markers in the GGA3 QTL *Growth4***
374 In the QTL *Growth4* on GGA3 (Figure 1; 24.0-68.1 Mb), both the association and linkage
375 analyses find the strongest signals between 24-41 Mb. Although the statistical support curve
376 in the linkage-analysis contains multiple peaks, that analysis was unable to fine-map the
377 region into multiple, independent signals. The association-analysis, however, revealed at least
378 two distinct association-peaks with several associated markers in each region. These regions
379 are located approximately 10 Mb apart and are separated by a region with very low
380 association. The regions are mapped with high resolution and are located approximately
381 between 24-27 Mb and 34-37 Mb, respectively. A candidate mutation in *Growth4* was found
382 slightly outside the second association region at 33.6 Mb inside the regulatory region of
383 Cystein rich transmembrane BMP regulator 1 *(CRIM1)* (Ahsan *et al.* 2013). In addition to the
384 two peaks described above, several nominally significant markers were located around 55-57
385 Mb, suggesting that also this region is associated with BW56. This is supported by the
386 forward-selection/backward-elimination analyses where the highly associated marker at 57.6
387 Mb is defined as experiment-wide significant. In the previously performed linkage-based
388 analysis, this region displayed very low significance.
389

Four statistically independent associated markers in the GGA20 QTL *Growth12*

The earlier linkage-analysis replicated the QTL *Growth12* on GGA20 (Figure 1: 7.1-13.9 Mb), with the strongest associated marker at 10.7 Mb, and the signal covered most of the region (8-13.9 Mb). In the association-analysis, several markers reached the nominal threshold and these are part of a focused association peak covering the region around 9 Mb and the region around 11 Mb. Both regions were identified as independent peaks in the backward-elimination analysis, suggesting that this QTL contains multiple associated loci.

Five statistically independent associated markers in the GGA4 QTLs *Growth6 and Growth7*

In both *Growth6* (Figure 1; 1.3-13.6 Mb) and *Growth7* (Figure 1.; 85.4-88.9 Mb) on GGA4, several markers were nominally significant in the association analysis. These markers were located very close to the main peaks in the earlier linkage-based analysis, suggesting that the two analyses identify the same underlying loci. The association analysis highlighted a region in *Growth7* with strong association around 86 Mb that was not found with the linkage-based approach. As for *Growth12*, this suggests that the *Growth7* also contains multiple associated loci.

General comments

Here we report the results from using an imputation-based association-mapping strategy to fine-map QTL in a nine-generation, outbred Advanced Intercross Line (AIL). By combining high-density genotyping of the AIL founders with imputation throughout the rest of the pedigree utilizing a sparser genotyped marker-backbone, we increased the marker-density ~20-fold in the studied regions. This subsequent association analysis had a comparable power for replication of QTL to the earlier used linkage-based strategy. In addition to this, the new

415 analyses also detected multiple association-peaks in several of the QTL and narrowed the
416 associated regions considerably compared to the regions detected previously (Besnier *et al.*
417 2011). Together, they suggest that this imputation-based association-mapping approach is a
418 promising strategy for improving the resolution in fine-mapping studies in outbred pedigrees,
419 where high-density marker genotypes are not available for all studied individuals.
420
421 In both *Growth1* and *Growth4* two strong, distinct association signals were identified. Also in
422 the QTL *Growth8* and *Growth9* the new analysis identified strong association-peaks covering
423 many markers. In these regions, the strongest linkage-signals identified in the previous fine-
424 mapping analysis (Besnier *et al.* 2011) overlap with the strongest signals in the current
425 analyses. However, the association analysis also separates the signals into multiple peaks and
426 highlights narrower regions. Hence, it provides more useful input for further analyses to
427 identify candidate genes underlying the QTL. In most cases the associated regions are
428 restricted to distinct 2-3 Mb regions, which as indicated by the findings from Ahsan *et al.*
429 (2013), is useful for restricting the bioinformatics analyses to only the most promising
430 candidate genes for further functional studies. The additive effect of the marker identified as
431 experiment-wide significant at 18.5 Mb in *Growth9* was assessed as transgressive. This,
432 together with the extended linkage signal and the problem to replicate the QTL through
433 introgression (Ek *et al.* 2012) suggests that the genetic architecture of the original *Growth9*
434 QTL is more complex than previously noted, potentially due to the effects of more than two
435 linked loci.
436
437 In *Growth6*, *Growth7*, and *Growth12*, the association signals were not as significant as in the
438 other QTL. Despite this, the multi-locus analyses suggest that the linkage signals in the earlier

439 analyses were due to distinct loci with independent effects, mapped here into narrower
440 association peaks.
441
442 Overall, the location of the association-signals in this study overlapped well with the top
443 signals in the earlier linkage analyses. However, in two of the QTL (*Growth2* and *Growth3*),
444 the association peaks are shifted when comparing results from the two studies. Further work
445 is needed to explore whether this reflects separate loci with distinct genetic architectures that
446 could only be detected with the respective methods, or if they reflect a signal of the same
447 underlying causal locus.
448
449 In the original study of (Jacobsson *et al.* 2005), the total effects of all significant and
450 suggestive QTL on BW56 was 634 g, corresponding to 47.3% of the difference between the
451 parental selected lines. Here, the combined effect of the markers retained in the multi-locus
452 model (Table 2) is 527 g. However, when considering only the QTL in the original study that
453 have been replicated here, their originally estimated contribution was 416 g, indicating that
454 the segregation of the QTL alleles in the founder-lines revealed here biased the originally
455 reported estimates that assumed fixation for alternative alleles in the HWS and LWS lines,
456 downwards. The allele-frequencies for the selected markers in the HWS founders show an
457 interesting pattern (Supplementary table 1). Although the weight-increasing alleles are more
458 common in the HWS at all markers, the alternative alleles are still far from fixation in the
459 lines. This suggests that multiple alleles are segregating both within and across the selected
460 lines at the loci with the largest individual effects in the population.
461
462 A key for successful imputation of the high-density marker set throughout the AIL pedigree is
463 that the haplotypes across these markers are correctly estimated in the founders. There are

464 several properties of the Virginia-lines that improve haplotype-estimation from high-density
465 genotypes. First, as the number of generations since the lines diverged is relatively few (40
466 generations), most new haplotypes will result from recombination of original haplotypes,
467 rather than by new mutations. Second, the strong artificial selection imposed on the
468 populations since they were founded is likely to have further reduced haplotype-diversity
469 across the genome. This is likely the reason that many selective-sweeps across long
470 haplotypes have been found to be fixed, or nearly fixed, across the genome within and
471 between the lineages (Johansson *et al.* 2010; Pettersson *et al.* 2013). This is reflected in a
472 large average LD-block size (> 50 kb) across the genome (Marklund and Carlborg 2010).
473 Given the density of the 60k SNP-chip genotyping used here, several markers will be present
474 on each such LD-block and hence improve efficiency in haplotype estimation. Additional
475 genotyping will, however, be necessary in subsequent generations to experimentally confirm
476 the associations to imputed markers reported here.
477
478 Genotype data is available for all individuals in the AIL pedigree. The dense marker
479 backbone (~1 marker/cM) from the first genotyping of the AIL (Besnier *et al.* 2011), allow
480 the relatively long haplotypes that are inherited as intact segments from parents to offspring to
481 be efficiently phased, imputed and traced throughout the pedigree for later association
482 analyses.
483
484 Here, the association-analysis was performed using a linear model including fixed effects of
485 genotype, sex and AIL generation. Sex and generation were included as both these
486 environmental factors had significant effects on BW56 (Besnier *et al.* 2011). Implementing
487 the model-selection by backward-elimination in a bootstrap-based framework is a way to
488 account for possible effects of population-structure in the AIL that might increase the risk for

reporting false positives. However, since the association signals in most cases overlap well with the final marker set resulting from the testing of experiment-wide significant associations, we do not find this to be any cause of great concern in this experiment.

Conclusion

In conclusion, this study shows that the proposed imputation-based association-mapping strategy, and further model selection by backward-elimination in a bootstrap-based framework, is useful for identifying independent association signals within and across the nine evaluated QTL. The association-peaks were narrower than those obtained in the earlier performed linkage analysis, often highlighting regions down to 2-3 Mb in length allowing the identification of multiple association-signals in several QTL. This suggests that the association-based strategy has higher resolution, as well as provides an improved power to disentangle the effects of multiple linked loci inside QTL, compared to linkage-based fine-mapping. Combining traditional linkage-based approaches to analyze outbred Advanced Intercross populations with imputation-based association mapping approaches might thus be an important and cost-effective approach to improve the efficiency in post-association bioinformatic analyses and functional explorations aiming to identify candidate mutations. A previous candidate-gene study based on the nine QTL fine-mapped here have already reported some interesting mutations in growth related genes (Ahsan *et al.* 2013) overlapping with the association signals reported here. Further bioinformatic investigations of the regions fine-mapped here could potentially reveal new important genes and mutations affecting body-weight in these chicken lines and provide new candidate genes for studying the genetic architecture of metabolic traits in other species, including humans.

AUTHORS' CONTRIBUTIONS

ÖC and PBS initiated the study. ÖC designed the project with MA and MB; PBS developed the Virginia chicken lines; PBS (with others) designed, planned and bred the Virginia Advanced Intercross Line; PBS and CFH designed, planned, bred, bled, phenotyped and extracted DNA from the Virginia Advanced Intercross Line population; ÖC designed the statistical analyses; MA, MB and ÖC contributed analysis scripts; ÖC, MB and MA performed the data analyses, summarized the results and wrote the manuscript. All authors read and approved the final manuscript.

ACKNOWLEDGEMENTS

Formas (grant 221-2013-450 to ÖC) and the Swedish Research Council (grant 621-2012-4634 to ÖC) are acknowledged for financial support. We thank Leif Andersson for initiating the AIL experiment with PBS and sharing the data from the F2 intercross. Per Wahlberg and Francois Besnier are acknowledged for their valuable contributions during preparation and quality control work of the genotype and phenotype data from the AIL. Genotyping was performed by the SNP&SEQ Technology Platform in Uppsala, which is part of Science for Life Laboratory at Uppsala University and is supported as a national infrastructure by the Swedish Research Council (VR-RFI).

REFERENCES

Abramovich F., Benjamini Y., Donoho D. L., Johnstone I. M., 2006 Special Invited Lecture: Adapting to Unknown Sparsity by Controlling the False Discovery Rate. The Annals of Statistics **34**: 584–653.

Ahsan M., Li X., Lundberg A. E., Kierczak M., Siegel P. B., Carlborg Ö., Marklund S., 2013 Identification of candidate genes and mutations in QTL regions for chicken growth using bioinformatic analysis of NGS and SNP-chip data. Front Genet **4**: 226.

539 Andersson L., 2001 Genetic dissection of phenotypic diversity in farm animals. Nat Rev
540 Genet **2**: 130–138.

541 Andersson L., Georges M., 2004 Domestic-animal genomics: deciphering the genetics of
542 complex traits. Nat Rev Genet **5**: 202–212.

543 Aulchenko Y. S., Ripke S., Isaacs A., van Duijn C. M., 2007 GenABEL: an R package for
544 genome-wide association analysis. Bioinformatics **23**: 1294–1296.

545 Benjamini Y., Hochberg Y., 1995 JSTOR: Journal of the Royal Statistical Society. Series B
546 (Methodological), Vol. 57, No. 1 (1995), pp. 289-300. Journal of the Royal Statistical
547 Society, Series B.

548 Besnier F., Wahlberg P., Rönnegård L., Ek W., Andersson L., Siegel P. B., Carlborg Ö., 2011
549 Fine mapping and replication of QTL in outbred chicken advanced intercross lines. Genet
550 Sel Evol **43**: 3.

551 Carlborg Ö., Jacobsson L., Åhgren P., Siegel P., Andersson L., 2006 Epistasis and the release
552 of genetic variation during long-term selection. Nat Genet **38**: 418–420.

553 Cheng R., Lim J. E., Samocha K. E., Sokoloff G., Abney M., Skol A. D., Palmer A. A., 2010
554 Genome-Wide Association Studies and the Problem of Relatedness Among Advanced
555 Intercross Lines and Other Highly Recombinant Populations. Genetics **185**: 1033–1044.

556 Daetwyler H. D., Wiggans G. R., Hayes B. J., Woolliams J. A., Goddard M. E., 2011
557 Imputation of missing genotypes from sparse to high density using long-range phasing. (I
558 Hoeschele, Ed.). Genetics **189**: 317–327.

559 Dunnington E. A., Siegel P. B., 1996 Long-term divergent selection for eight-week body
560 weight in white Plymouth rock chickens. Poultry science **75**: 1168–1179.

561 Dunnington E. A., Honaker C. F., McGilliard M. L., Siegel P. B., 2013 Phenotypic responses
562 of chickens to long-term, bidirectional selection for juvenile body weight--historical
563 perspective. Poultry science **92**: 1724–1734.

564 Ek W., Marklund S., Ragavendran A., Siegel P., Muir W., Carlborg Ö., 2012 Generation of a
565 multi-locus chicken introgression line to study the effects of genetic interactions on
566 metabolic phenotypes in chickens. Front Genet **3**: 29.

567 Gavrilov Y., Benjamini Y., Sarkar S. K., 2009 An Adaptive Step-Down Procedure with
568 Proven Fdr Control Under Independence. The Annals of Statistics **37**: 619–629.

569 Hill W., 2005 A century of corn selection. Science **307**: 683–684.

570 Jacobsson L., Park H.-B., Wahlberg P., Fredriksson R., Perez-Enciso M., Siegel P. B.,
571 Andersson L., 2005 Many QTLs with minor additive effects are associated with a large
572 difference in growth between two selection lines in chickens. Genet. Res. **86**: 115–125.

573 Johansson A. M., Pettersson M. E., Siegel P. B., Carlborg Ö., 2010 Genome-Wide Effects of
574 Long-Term Divergent Selection. PLoS Genet **6**: e1001188.

575 Le Rouzic A., Carlborg Ö., 2008 Evolutionary potential of hidden genetic variation. Trends in
576 Ecology & Evolution **23**: 33–37.

577 Le Rouzic A., Siegel P. B., Carlborg Ö., 2007 Phenotypic evolution from genetic
578 polymorphisms in a radial network architecture. BMC Biol. **5**: 50.

579 Marklund S., Carlborg Ö., 2010 SNP detection and prediction of variability between chicken
580 lines using genome resequencing of DNA pools. BMC Genomics **11**: 665.

581 Márquez G. C., Siegel P. B., Lewis R. M., 2010 Genetic diversity and population structure in

582 lines of chickens divergently selected for high and low 8-week body weight. Poultry
583 science **89**: 2580–2588.

584 Park H.-B., Jacobsson L., Wahlberg P., Siegel P. B., Andersson L., 2006 QTL analysis of
585 body composition and metabolic traits in an intercross between chicken lines divergently
586 selected for growth. Physiological Genomics **25**: 216–223.

587 Peirce J. L., Broman K. W., Lu L., Chesler E. J., Zhou G., Airey D. C., Birmingham A. E.,
588 Williams R. W., 2008 Genome Reshuffling for Advanced Intercross Permutation
589 (GRAIP): Simulation and Permutation for Advanced Intercross Population Analysis (WE
590 Crusio, Ed.). PLoS ONE **3**: e1977.

591 Pettersson M. E., Johansson A. M., Siegel P. B., Carlborg Ö., 2013 Dynamics of Adaptive
592 Alleles in Divergently Selected Body Weight Lines of Chickens. G3 (Bethesda) **3**: 2305–
593 2312.

594 Pettersson M., Besnier F., Siegel P. B., Carlborg Ö., 2011 Replication and explorations of
595 high-order epistasis using a large advanced intercross line pedigree. PLoS Genet **7**:
596 e1002180.

597 R Development Core Team, 2015 *R: A Language and Environment for Statistical Computing*.
598 Vienna, Austria.

599 Rönnegård L., Besnier F., Carlborg Ö., 2008 An improved method for quantitative trait loci
600 detection and identification of within-line segregation in F2 intercross designs. Genetics
601 **178**: 2315–2326.

602 Sheng Z., Pettersson M. E., Honaker C. F., Siegel P. B., Carlborg Ö., 2015 Standing genetic
603 variation as a major contributor to adaptation in the Virginia chicken lines selection

experiment. Genome Biol. **16**: 219.

Valdar W., Holmes C. C., Mott R., Flint J., 2009 Mapping in structured populations by resample model averaging. Genetics **182**: 1263–1277.

Wahlberg P., Carlborg Ö., Foglio M., Tordoir X., Syvänen A.-C., Lathrop M., Gut I. G., Siegel P. B., Andersson L., 2009 Genetic analysis of an F(2) intercross between two chicken lines divergently selected for body-weight. BMC Genomics **10**: 248.

Table S1.

GGA [a]	QTL [b]	Position [c] (bp)	Marker [d]	a ± SE [e]	Sign. [f]	p HWS [g]	p LWS [h]	MAF F2-F8 [i]
1	Growth1	173 709 608	rs14916997	-36.6 ± 5.5	3.6×10^{-11}	0.11	0.82	0.48
		179 613 655	rs313927704	41.6 ± 12.2	6.5×10^{-4}	0.30	0.04	0.05
		170 637 618	rs13968052	19.1 ± 6.6	3.8×10^{-3}	0.35	0.07	0.21
		176 383 356	rs13975251	19.7 ± 7.7	1.1×10^{-2}	0.43	0.09	0.12
		178 029 363	rs317567034	-31.6 ± 11.6	6.4×10^{-3}	0.20	0.02	0.05
		179 806 129	rs314200699	28.8 ± 12.2	1.8×10^{-2}	0.04	0.14	0.05
		169 810 898	rs15487296	161.7 ± 78.5	4.0×10^{-2}	0.00	0.34	0.00
2	Growth2	64 317 336	rs14194723	-101.5 ± 15.9	1.5×10^{-10}	0.04	0.04	0.03
		62 837 662	rs14192893	458.6 ± 138.1	9.0×10^{-4}	0.02	0.00	0.00
		59 778 572	rs316345242	-28.7 ± 9.2	1.8×10^{-3}	0.20	0.02	0.09
		56 720 515	rs14185295	15.3 ± 5.5	5.2×10^{-3}	0.46	0.14	0.39
		54 865 875	rs14183473	57.4 ± 20.3	4.7×10^{-3}	0.00	0.30	0.02
		57 198 629	rs14185836	-14.1 ± 5.4	9.7×10^{-3}	0.41	0.25	0.39
		65 460 002	rs14196021	14.4 ± 6.0	1.7×10^{-2}	0.43	0.11	0.25
		55 330 630	rs15100427	13.7 ± 6.4	3.2×10^{-2}	0.37	0.34	0.21
		62 639 245	rs15107150	-74.8 ± 36.2	3.9×10^{-2}	0.11	0.00	0.00
2	Growth3	130133780	rs14248248	20.2 ± 6.5	1.9×10^{-3}	0.07	0.57	0.21
		130 592 117	rs16133110	-62.2 ± 25.4	1.4×10^{-2}	0.00	0.11	0.01
		126 000 254	rs16120360	13.8 ± 6.1	2.3×10^{-2}	0.54	0.18	0.28
3	Growth4	37 287 334	rs316425755	-32.6 ± 6.4	2.9×10^{-7}	0.26	0.38	0.23
		26 215 175	rs14328509	-21.8 ± 5.4	5.1×10^{-5}	0.26	0.79	0.45
		28 981 759	rs313368484	92.5 ± 24.7	1.8×10^{-4}	0.02	0.16	0.01
		36 103 180	rs13723817	26.3 ± 6.8	1.0×10^{-4}	0.02	0.55	0.18
		57 624 596	rs14363139	-18.0 ± 5.2	5.7×10^{-4}	0.13	0.77	0.50

		61 227 711	rs16284878	-34.6 ± 11.0	1.6×10^{-3}	0.59	0.09	0.06
		47 729 342	rs316384373	21.9 ± 6.9	1.6×10^{-3}	0.04	0.34	0.16
		53 589 855	rs14359071	34.7 ± 11.9	3.5×10^{-3}	0.37	0.27	0.05
		60 099 912	rs14364587	-33.2 ± 11.2	3.0×10^{-3}	0.57	0.00	0.06
		39 139 081	rs15468467	-16.6 ± 6.4	9.2×10^{-3}	0.15	0.38	0.21
		33 743 569	rs314044798	15.6 ± 5.0	1.9×10^{-3}	0.09	0.55	0.38
		40 789 962	rs16256006	-53.8 ± 20.0	7.2×10^{-3}	0.04	0.00	0.01
		38 049 506	rs14341458	72.7 ± 26.2	5.6×10^{-3}	0.09	0.00	0.01
		36 036 392	rs14339632	29.3 ± 10.7	6.1×10^{-3}	0.00	0.11	0.05
		53 236 895	rs13570951	-17.9 ± 7.1	1.2×10^{-2}	0.52	0.05	0.10
		49 677 389	rs15350215	55.0 ± 21.0	8.9×10^{-3}	0.17	0.00	0.01
		24 558 483	rs14326932	-180.3 ± 75.5	1.7×10^{-2}	0.00	0.20	0.00
		52 685 153	rs13570803	14.0 ± 5.8	1.7×10^{-2}	0.33	0.68	0.20
		61 496 004	rs315203852	24.7 ± 10.3	1.6×10^{-2}	0.57	0.00	0.06
		25 074 560	rs14327473	41.5 ± 19.5	3.3×10^{-2}	0.22	0.11	0.02
		50 259 236	rs14356142	-46.7 ± 22.5	3.8×10^{-2}	0.00	0.16	0.01
4	Growth6	13 511 203	rs15500313	25.4 ± 5.5	3.3×10^{-6}	0.91	0.13	0.46
		10 914 312	rs14428120	17.3 ± 5.3	1.1×10^{-3}	0.07	0.84	0.43
		2 392 397	rs14419462	23.4 ± 8.1	3.8×10^{-3}	0.35	0.05	0.13
		1 379 849	rs314301286	-42.3 ± 13.3	1.5×10^{-3}	0.04	0.07	0.04
		3 589 044	rs10732133	-36.6 ± 11.1	9.4×10^{-4}	0.28	0.04	0.06
		4 908 910	rs14422558	-151.2 ± 55.9	6.9×10^{-3}	0.00	0.11	0.00
		11 693 052	rs314301286	37.0 ± 14.8	1.3×10^{-2}	0.07	0.18	0.03
		11 345 880	rs14428501	-22.5 ± 9.2	1.4×10^{-2}	0.02	0.34	0.09
		2 850 506	rs14420072	49.5 ± 22.0	2.5×10^{-2}	0.00	0.09	0.01
4	Growth7	88 325 118	rs15639000	-21.0 ± 5.4	9.9×10^{-5}	0.46	0.52	0.47
		86 755 267	rs14499758	-28.0 ± 6.3	7.9×10^{-6}	0.11	0.43	0.26
		87 755 983	rs318052788	21.0 ± 8.9	1.8×10^{-2}	0.04	0.18	0.09

		87 290 961	rs14500395	-286.6 ± 138.1	3.8×10^{-2}	0.00	0.02	0.00
5	Growth8	36 291 277	rs13585490	-32.9 ± 5.3	4.5×10^{-10}	0.39	0.54	0.40
		38 774 986	rs315605733	-29.6 ± 6.5	5.8×10^{-6}	0.04	0.27	0.19
		35 299 978	rs16487933	-19.9 ± 6.2	1.2×10^{-3}	0.65	0.25	0.24
		36 426 195	rs15697504	-49.3 ± 16.0	2.0×10^{-3}	0.22	0.46	0.03
		38 867 279	rs314075508	-12.6 ± 4.9	1.1×10^{-2}	0.09	0.46	0.48
		36 575 445	rs16489220	-43.4 ± 17.5	1.3×10^{-2}	0.15	0.48	0.02
		34 772 650	rs16487762	14.0 ± 7.0	4.6×10^{-2}	0.67	0.14	0.17
		33 713 055	rs14530756	11.5 ± 5.3	3.2×10^{-2}	0.22	0.68	0.35
7	Growth9	23 959 214	rs16596357	-38.9 ± 5.4	7.1×10^{-13}	0.33	0.50	0.34
		26 021 398	rs14618036	80.8 ± 22.6	3.6×10^{-4}	0.11	0.00	0.01
		18 544 622	rs14611566	18.3 ± 5.3	5.8×10^{-4}	0.50	0.50	0.46
		33 699 148	rs16610251	67.0 ± 23.0	3.5×10^{-3}	0.24	0.04	0.01
		32 262 733	rs317586448	-15.1 ± 5.2	3.4×10^{-3}	0.74	0.41	0.44
		27 518 867	rs14619679	32.7 ± 12.1	6.8×10^{-3}	0.09	0.09	0.05
		29 631 963	rs10727581	17.2 ± 6.2	5.4×10^{-3}	0.39	0.07	0.22
		29 999 307	rs14622731	-30.3 ± 10.6	4.3×10^{-3}	0.26	0.00	0.06
		23 134 876	rs312633887	-30.8 ± 12.0	1.0×10^{-2}	0.41	0.18	0.05
		35 390 789	rs317022486	-25.2 ± 10.0	1.2×10^{-2}	0.15	0.30	0.07
		14 071 039	rs16088281	34.6 ± 15.8	2.9×10^{-2}	0.02	0.09	0.03
		25 726 731	rs317769956	-22.5 ± 9.0	1.2×10^{-2}	0.00	0.34	0.09
		24 549 929	rs14616465	-101.8 ± 50.3	4.3×10^{-2}	0.00	0.11	0.00
20	Growth12	10 667 729	rs16172598	26.3 ± 5.4	1.1×10^{-6}	0.67	0.11	0.33
		10 965 403	rs16173231	346.1 ± 139.1	1.3×10^{-2}	0.04	0.00	0.00
		8 814 245	rs314843162	21.9 ± 8.8	1.3×10^{-2}	0.24	0.11	0.09
		13 427 530	rs16176151	-13.9 ± 5.2	7.0×10^{-3}	0.35	0.48	0.48
		7 881 700	rs312541071	-73.1 ± 29.7	1.4×10^{-2}	0.20	0.07	0.01
		11 389 861	rs13634923	19.2 ± 8.3	2.1×10^{-2}	0.24	0.20	0.11

10 165 171	rs14278292	-12.7 ± 5.8	2.9×10^{-2}	0.50	0.13	0.26
9 302 754	rs14277526	14.1 ± 6.1	2.0×10^{-2}	0.39	0.05	0.23

Statistically suggestive independent signals within each QTL identified as nominally significant ($p < 0.05$) in the forward-selection procedure. For each QTL, Model 1 was first fitted for all markers and the most significant marker was selected and added as a covariate before refitting model 1 again. This procedure, selecting the most significant marker as a covariate and refitting Model 1, was repeated until no markers within the QTL reached the nominal significance threshold.

[a] Gallus Gallus Autosome; [b] QTL name as in (Jacobsson et al. 2005); [c] Base pair position according to *Chicken* genome assembly (galGal3) of May 2006; [d] SNP name as in NCBI dbSNP; [e] Additive effect ± Standard Error calculated within each QTL as described in model 1; [f] Significance of the estimated additive genetic effect from fitting model 1; [g] Frequency of the allele corresponding to the estimated effect, calculated from all founder birds which originates from the high-weight selection line; [h] Frequency of the allele corresponding to the estimated effect, calculated from all founder birds which originates from the low-weight selection line; [i] Minor allele frequency calculated from all 1348 birds , AIL generation F2-F8, included in the study.